Forward-backward asymmetry induced *CP* asymmetry of $B^{\pm} \to \pi^{\pm}\pi^{+}\pi^{-}$

Ya-Rui Wei and Zhen-Hua Zhang*

School of Nuclear Science and Technology, University of South China, Hengyang, Hunan 421001, China

(Received 7 September 2022; accepted 18 November 2022; published 12 December 2022)

CP violation of the decay $B^{\pm} \to \pi^{\pm}\pi^{+}\pi^{-}$ in the $f_0(500) - \rho(770)^0$ interfering region is analyzed. The forward-backward asymmetries (FBAs) and the corresponding *CP* asymmetries FB-*CP*As are particularly investigated. To isolate the *CP*V caused by the interference of different partial wave more cleanly, we also introduce the direct-*CP*V-subtracted FB-*CP*A. Based on the LHCb data, we extract the FBAs, FB-*CP*As, direct-*CP*V-subtracted FB-*CP*A, as well as the regional *CP*As with invariant mass of the $\pi^{+}\pi^{-}$ pair in the range $0.2\ \mathrm{GeV}/c^2 < \sqrt{s_{\mathrm{low}}} < 1.8\ \mathrm{GeV}/c^2$. It is found that the (direct-*CP*V-subtracted) FB-*CP*As are quite large in the $f_0(500) - \rho(770)^0$ interfering region, which confirms that the interference of the intermediate resonances $f_0(500)$ and $\rho(770)^0$ plays an important role for the *CP* violation of the three-body decay channel $B^{\pm} \to \pi^{\pm}\pi^{+}\pi^{-}$.

DOI: 10.1103/PhysRevD.106.113002

I. INTRODUCTION

Charge-parity (*CP*) violation was discovered by J.W. Cronion and V.L. Fitch in the neutral kaon system in 1964 [1]. It is closely related to the matter-antimatter symmetry in our universe [2], and is one of the most basic and important properties of the weak interaction. In the Standard Model (SM), *CP* violation (*CP*V) results from the weak complex phase in the Cabibbo-Kobayashi-Maskawa (CKM) matrix that reflects the transitions of different generations of quarks [3,4]. To date, *CP*V has been observed in the K, B, and D meson systems [1,5–11], all of which are consistent with the KM mechanism of SM [4].

The study on *CP*V in multi-body decays of the bottom and the charmed hadrons plays an increasingly important role in both testing the KM mechanism of SM and looking for new sources of *CP*V. Interestingly, large *CP* asymmetries (*CP*As) regionalized in part of the phase space in some three-body decay channels of B mesons have been reported by LHCb [12–15]. Meanwhile, the integrated *CP*As are relatively small due to the cancellation among different parts of the phase space. Among these three-body decay channels, $B^{\pm} \to \pi^{\pm}\pi^{+}\pi^{-}$ is one of the most extensively studied. Amplitude analysis of this decay channel shows that $\rho(770)^0$ is the dominant resonance [16–19]. The large regional *CP*A observed by LHCb located right in part of the $\rho(770)^0$ region where the angle (in the rest frame of $\rho(770)^0$) of the two pions with the same charge with B—which will be denoted as θ in this paper—is smaller that 90^0 [13,14]. Theoretical analysis indicates that the aforementioned large regional *CP*A can be explained by the interference of $\rho(770)^0$ with the nearby resonance $f_0(500)$, where the corresponding amplitudes are respectively P- and S-waves [20–25]. The interference behavior around $\rho(770)^0$ can be well explained based on a QCD factorization approach for the weak amplitude of $B^{-} \to \rho(770)^0\pi^{-}$ and $B^{-} \to f_0(500)\pi^{-}$ [26].

Although it can be well explained by the interference of $f_0(500)$ and $\rho(770)^0$, the large regional *CP*A in $B^{\pm} \to \pi^{\pm}\pi^{+}\pi^{-}$ entangles all kinds of contributions other than the aforementioned $f_0(500) - \rho(770)^0$ interference, such as contributions from interference between the tree and penguin part corresponding to $\rho(770)^0$. Recently, one of the authors (Z.H.Z.) has proposed to study *CP*V induced by the interference of the nearby resonance through the forward-backward asymmetry (FBA) of the final particle and the FBA induced *CP* Asymmetry (FB-*CP*A) [27]. One advantage of this method is that it can isolated *CP*V caused by the interfering effect of the nearby resonances (respectively corresponding to even- and odd-waves) [28].

The large data sample allows LHCb to study the *CP*V caused by the interference of the S- and P-waves in more detail. To do this, the event yields are allocated into bins according to $\cos\theta > 0$ or $\cos\theta < 0$. In this way, the corresponding regional *CP*As can be systematics studied [13]. However, the analysis of the FBAs and the FB-*CP*As is absent in the LHCb's previous works. This motivates us to performed the analysis of the FBAs and the

*zhangzh@usc.edu.cn

FB-CPAs of $B^{\pm} \to \pi^{\pm}\pi^{+}\pi^{-}$ in this paper, based on the LHCb's data in Refs. [13] and [14].

This paper is organized as follows. In Sec. II, we first illustrate the definitions of FBA and FB-CPA in detail. In Sec. III, based on the data sample corresponding to an integrated luminosity of 3.0 fb^{-1} collected by the LHCb detector [13], we extract the regional CPAs, the FBAs, the FB-CPAs, as well as the newly introduced CP observables direct-CPV-subtracted FB-CPAs. A fit of $\cos\theta$-dependence of CPA with only the inclusion of the amplitudes corresponding to $f_0(500)$ and $\rho(770)^0$ is presented at the end of this section. In Sec. IV, we briefly give the conclusion.

II. THE FORWARD-BACKWARD ASYMMETRY INDUCED CP ASYMMETRY

We first illustrate the definition of several CPA observables for the decay process $B^- \to \pi^-\pi^+\pi^-$. In the c. m. frame of one of the $\pi^+\pi^-$ pair with low invariant mass, the aforementioned angle θ between the two π^-'s are illustrated in Fig. 1. In practice, the invariant mass of the $\pi^+\pi^-$ pair is separated into small intervals. For each interval, it can be further separated into two small regions according to $\cos\theta > 0$ or $\cos\theta < 0$, which will be denoted as Ω_i^+ or Ω_i^-, respectively, where the subscript i is the label of the small interval. The regional CPAs, which have been repeatedly dealt with in the literature both theoretically and experimentally, are defined as

$$A_{CP}^{\Omega_i^{\pm}} = \frac{N_{\Omega_i^{\pm}} - \bar{N}_{\Omega_i^{\pm}}}{N_{\Omega_i^{\pm}} + \bar{N}_{\Omega_i^{\pm}}}, \tag{1}$$

for the region $\Omega_i^{\pm}$, where $N_{\Omega_i^{\pm}}$ and $\bar{N}_{\Omega_i^{\pm}}$ are the event yields of $B^- \to \pi^-\pi^-\pi^+$ and $B^+ \to \pi^+\pi^+\pi^-$ in the region $\Omega_i^{\pm}$, respectively. Of course, the regional CPA for $\Omega_i \equiv \Omega_i^+ + \Omega_i^-$ is defined as

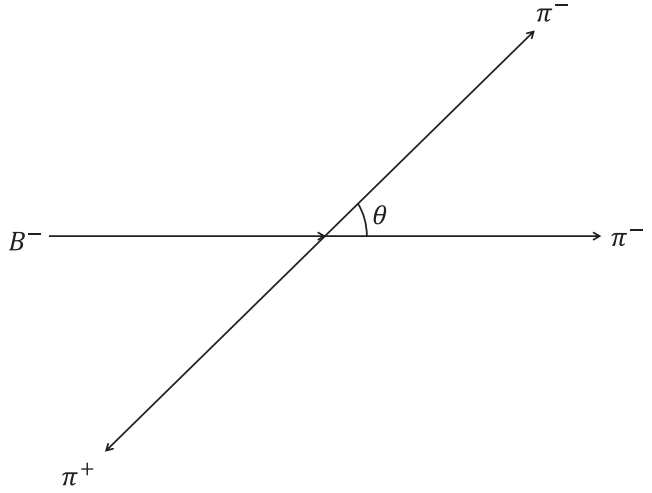

FIG. 1. The definition of θ.

$$A_{CP}^{\Omega_i} = \frac{N_{\Omega_i} - \bar{N}_{\Omega_i}}{N_{\Omega_i} + \bar{N}_{\Omega_i}}, \tag{2}$$

where N_{Ω_i} and $\bar{N}_{\Omega_i}$ are respectively the event yields of $B^- \to \pi^-\pi^-\pi^+$ and $B^+ \to \pi^+\pi^+\pi^-$ in Ω_i.

The FBA of the interval i of $B^- \to \pi^-\pi^+\pi^-$ is defined as the relative event yields difference between Ω_i^+ and Ω_i^-:

$$A_i^{FB} \equiv \frac{N_{\Omega_i^+} - N_{\Omega_i^-}}{N_{\Omega_i^+} + N_{\Omega_i^-}}. \tag{3}$$

The FB-CPA of the interval i is defined as

$$A_{CP,i}^{FB} = \frac{1}{2}(A_i^{FB} - \overline{A_i^{FB}}), \tag{4}$$

where $\overline{A^{FB}}$ represents the FBA of the interval i for $B^+ \to \pi^+\pi^+\pi^-$. Comparing with the regional CPAs, the FB-CPA is free from the assumption of equal production of B^- and B^+ [29], which reduces the corresponding systematic uncertainties.

Alternatively, one can define the CPA corresponding to FBA as $A_{CP,i}^{FB,\mathrm{alt}} = \frac{A_i^{FB} - \overline{A_i^{FB}}}{A_i^{FB} + \overline{A_i^{FB}}}$, which is similar with the CPAs defined by the decay width. However, there are good reasons for us not to use this definition here. Mathematically, since neither A^{FB} nor $\overline{A^{FB}}$ are positive-definite, the CPA defined in the above equation is not bounded in $(-1, 1)$. In other words, $A_{CP,i}^{FB}$ is normalized, while $A_{CP,i}^{FB,\mathrm{alt}}$ is not. To be more specific, $A_{CP,i}^{FB,\mathrm{alt}}$ is in fact the relative FB-CPA with respect to the CP-averaged FBA, $A_i^{FB,CP-\mathrm{av}} \equiv \frac{1}{2}(A_i^{FB} + \overline{A_i^{FB}})$, which can be clearly seen from a transformed expression: $A_{CP,i}^{FB,\mathrm{alt}} = A_{CP,i}^{FB}/A_i^{FB,CP-\mathrm{av}}$. Hence the aforementioned alternative definition is questionable when one want to make a comparison with other CPAs, such as the regional ones. From this perspective, the definition of Eq. (4) is more reasonable for the usage in this paper.[1]

[1]Similar story happens in other cases, such as the hyperon decays, where the CPA corresponding to the decay parameter α are defined in the literature as $A_{CP}^{\alpha} = \frac{\alpha+\bar{\alpha}}{\alpha-\bar{\alpha}}$, while an alternative definition which is similar with Eq. (4) was presented in Ref. [30]. According to the logic here, the former should be view as the relative α-induced CPA with respect to the CP-averaged decay parameter $\alpha^{CP-\mathrm{av}} \equiv \frac{1}{2}(\alpha - \bar{\alpha})$, while the latter is the α-induced CPA: $A_{CP}^{\alpha-\mathrm{ind}} \equiv \frac{1}{2}(\alpha + \bar{\alpha})$. Of course, we are not saying that the latter definition of CPA is better. On the contrary, despite non-normalized, the former does have some distinct advantages. For example, the former defined relative CPA can be measured through $\Lambda_c^+ \to \Lambda(\to p\pi^-)h^+$ [31,32] based only on the CP symmetry assumption for the decay $\Lambda_c^+ \to \Lambda h^+$ ($h^+ = K^+$ or π^+), while the latter cannot.

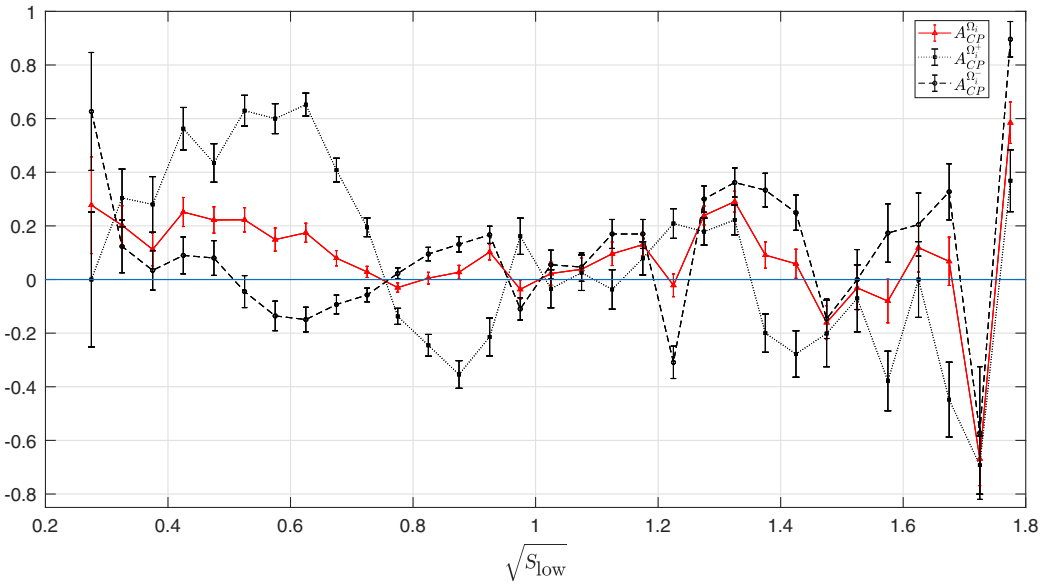

FIG. 2. The regional *CP*As, $A_{CP}^{\Omega_i^+}$, and $A_{CP}^{\Omega_i^-}$, and $A_{CP}^{\Omega_i}$ of the decay channel $B^\pm \to \pi^\pm\pi^+\pi^-$ extracted from the LHCb data in Ref. [13] for $\sqrt{s_{\rm low}}$ from 0.2 GeV/c^2 to 1.8 GeV/c^2. The dotted, dashed, and solid lines are $A_{CP}^{\Omega_i^+}$, $A_{CP}^{\Omega_i^-}$, and $A_{CP}^{\Omega_i}$, respectively.

The nonzero of FBA is caused by the interference of the odd- and even-waves [28]. To see this, one express the decay amplitude as

$$A = \sum_l a_l P_l(\cos\theta), \tag{5}$$

the FBA is then

$$A^{FB} = \frac{1}{\sum_j[\langle|a_j|^2\rangle/(2j+1)]} \sum_{\substack{\text{even } l \\ \text{odd } k}} f_{lk}\Re(\langle a_l a_k^*\rangle), \tag{6}$$

where $f_{lk} = \frac{(-)^{(l+k+1)/2} l!k!}{2^{l+k-1}(l-k)(l+k+1)[(l/2)!]^2\{[(k-1)/2]!\}^2}$ [33]. Consequently, the FB-*CP*A provide an effective procedure to isolate *CP*V corresponding to the interference of odd- and even-waves. Strictly speaking, however, the FB-*CP*A contains also *CP*Vs corresponding to the difference between the decay width of *CP*-conjugate processes. This can been seen from the denominator of the above equation, which is proportional to the decay width. Hence, the difference between the decay width of the *CP*-conjugate processes, which is in fact the origin of the direct *CP*V, can also contribute to FB-*CP*A. To eliminate this, one can introduce an observable, which will be called as the direct-*CP*V-subtracted FB-*CP*A, taking the form

$$\tilde{A}_{CP}^{FB} \equiv \frac{\sum_{\substack{\text{even } l \\ \text{odd } k}} f_{lk}\Re(\langle a_l a_k^*\rangle - \langle \bar{a}_l \bar{a}_k^*\rangle)}{\sum_j[\langle|a_j|^2\rangle/(2j+1)] + \sum_j[\langle|\bar{a}_j|^2\rangle/(2j+1)]}. \tag{7}$$

For the current situation, the direct-*CP*V-subtracted FB-*CP*A of the interval i can be expressed as

$$\tilde{A}_{CP,i}^{FB} = \frac{(N_{\Omega_i^+} - N_{\Omega_i^-}) - (\bar{N}_{\Omega_i^+} - \bar{N}_{\Omega_i^-})}{N_{\Omega_i} + \bar{N}_{\Omega_i}}, \tag{8}$$

based on the assumption that the B^- and B^+ are equally produced.

III. FBA AND FB-*CP*A ANALYSIS BASED ON LHCB DATA IN $B^\pm \to \pi^\pm\pi^+\pi^-$

Detailed analysis of the event distributions of the decay $B^\pm \to \pi^\pm\pi^+\pi^-$ has been performed by LHCb based on a data sample corresponding to an integrated luminosity of 3.0 fb^{-1} [13,14]. Based on the data in Ref. [13], we can extract the regional *CP*As, the FBAs, the FB-*CP*As, as well as the direct-*CP*V-subtracted FB-*CP*As in a wide region of the $\pi^+\pi^-$ pair with lower invariant mass: 0.2 GeV/c^2 < $\sqrt{s_{low}}$ < 1.8 GeV/c^2, which are presented in Figs. 2 and 3.

FIG. 2 shows the corresponding regional *CP*As of each bins with width of 0.05 GeV/c^2 lying in the range 0.2 GeV/c^2 < $\sqrt{s_{\rm low}}$ < 1.8 GeV/c^2, while Fig. 3 shows the FBAs, the FB-*CP*As, and the direct-*CP*V-subtracted FB-*CP*As. The errors are estimated with only the inclusion of the statistical uncertainties of the event yields estimated according to $\sqrt{N}$. Both of the two figures show interesting behavior around the $f_0(500) - \rho(770)^0$ interference region, i.e., 0.45 GeV/c^2 < $\sqrt{s_{\rm low}}$ < 0.75 GeV/c^2.

One can see from Fig. 2 that the regional *CP*As $A_{CP}^{\Omega_i^+}$ are quite large in the $f_0(500) - \rho(770)^0$ interference region. For the FBAs, the FB-*CP*As, and the direct-*CP*V-subtracted FB-*CP*As in Fig. 3, one can see that there

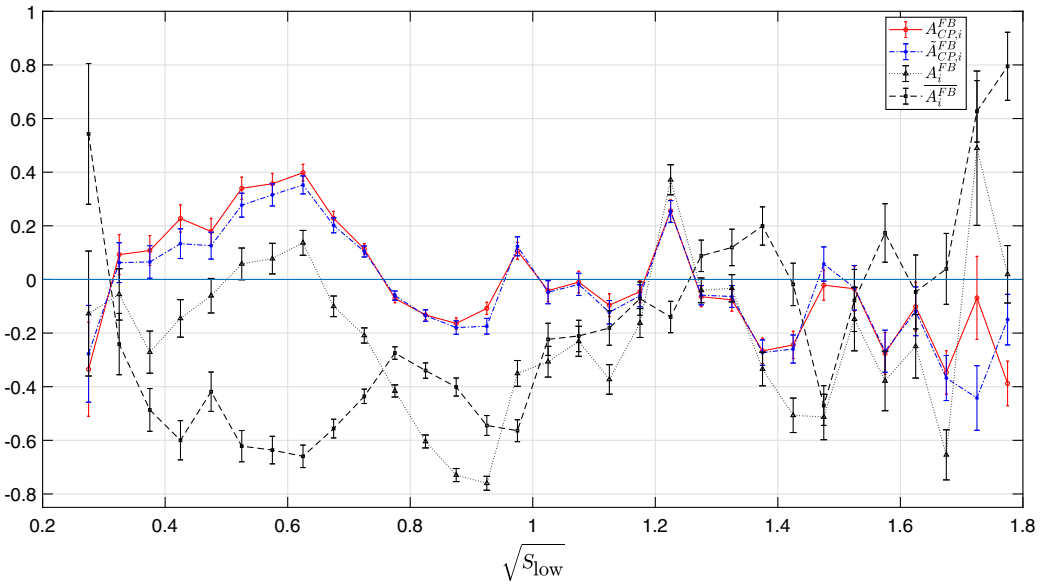

FIG. 3. The FBAs (A_i^{FB}), the FB-CPAs ($A_{CP,i}^{FB}$), and the direct-CPV-subtracted FB-CPAs ($\tilde{A}_{CP,i}^{FB}$) of the decay channel $B^{\pm} \to \pi^{\pm}\pi^{+}\pi^{-}$ for $\sqrt{s_{\rm low}}$ from 0.2 GeV/c^2 to 1.8 GeV/c^2. The dotted and dashed lines are A_i^{FB} and $\overline{A_i^{FB}}$, respectively. The solid and dash-dotted lines are $A_{CP,i}^{FB}$ and $\tilde{A}_{CP,i}^{FB}$, respectively.

are big differences between A_i^{FB} and $\overline{A_i^{FB}}$, resulting in a large $A_{CP,i}^{FB}$. For a more detailed and transparent comparison, we present all the five CPAs, $A_{CP}^{\Omega_i}$, $A_{CP}^{\Omega_i^+}$, $A_{CP}^{\Omega_i^-}$, $A_{CP,i}^{FB}$, and $\tilde{A}_{CP,i}^{FB}$ in Fig. 4.

The first thing one can see from Fig. 4 is that $A_{CP}^{\Omega_i^+}$, $A_{CP,i}^{FB}$, and $\tilde{A}_{CP,i}^{FB}$ are quite large throughout the whole $f_0(500) - \rho(770)^0$ interference region. Besides, the differences between $A_{CP}^{\Omega_i^+}$ and $A_{CP}^{\Omega_i^-}$ are very large too. However, when summed up the event yields of the region Ω_i, the resulting CPAs $A_{CP}^{\Omega_i}$ are much smaller. This means that the CP violation in this region is dominated by the interference of S- and P-waves amplitudes, i.e., the interference between the amplitudes corresponding to

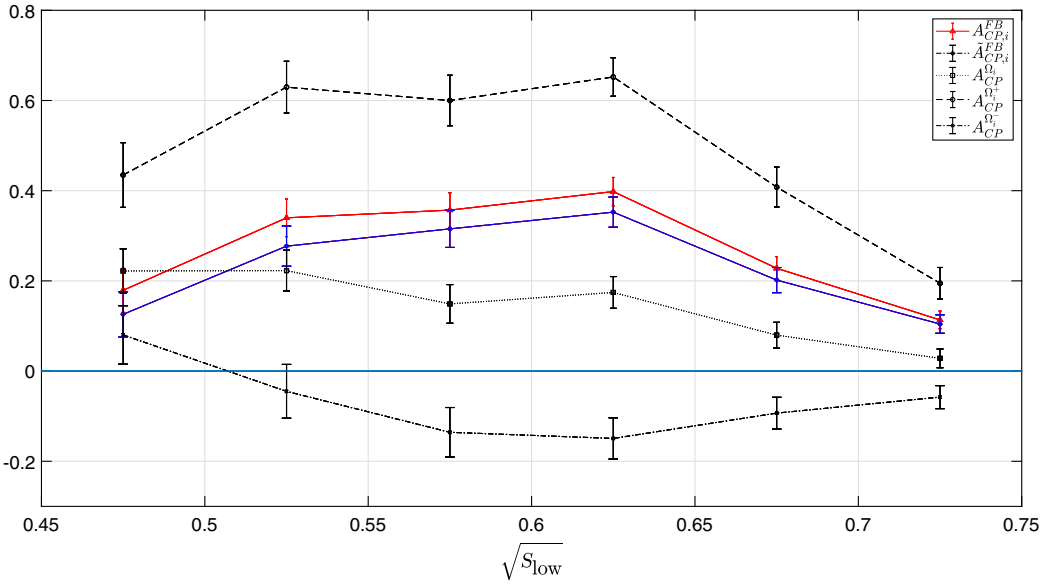

FIG. 4. The CPAs, $A_{CP,i}^{FB}$, $\tilde{A}_{CP,i}^{FB}$, $A_{CP}^{\Omega_i}$, $A_{CP}^{\Omega_i^+}$, and $A_{CP}^{\Omega_i^-}$ of the decay channel $B^{\pm} \to \pi^{\pm}\pi^{+}\pi^{-}$ for $\sqrt{s_{\rm low}}$ from 0.45 GeV/c^2 to 0.75 GeV/c^2. The upper and lower solid lines are $A_{CP,i}^{FB}$ and $\tilde{A}_{CP,i}^{FB}$, respectively. The dotted, dashed, and dash-dotted lines are $A_{CP}^{\Omega_i}$, $A_{CP}^{\Omega_i^+}$, and $A_{CP}^{\Omega_i^-}$, respectively.

TABLE I. The averaged CPAs, A_{CP}^{FB}, $\tilde{A}_{CP}^{FB}$, A_{CP}^{Ω}, $A_{CP}^{\Omega^+}$ and $A_{CP}^{\Omega^-}$ of the whole $f_0(500)-\rho(770)^0$ interference region, for 0.45 GeV/c^2 $<\sqrt{s_{\rm low}}<$ 0.75 GeV/c^2, where the uncertainties are statistical only.

A_{CP}^{FB}	$\tilde{A}_{CP}^{FB}$	A_{CP}^{Ω}	$A_{CP}^{\Omega^+}$	$A_{CP}^{\Omega^-}$
0.224 ± 0.012	0.194 ± 0.013	0.099 ± 0.013	0.405 ± 0.020	-0.074 ± 0.017

$f_0(500)$ and $\rho(770)^0$ respectively. This conclusion can also be verified from the small difference between $A_{CP,i}^{FB}$ and $\tilde{A}_{CP,i}^{FB}$, since their difference reflects the CPV *within* the S- or P-waves.

Amplitude analysis of this decay channel $B^\pm\to\pi^-\pi^+\pi^\pm$ showed that $\rho(770)^0$ plays a dominant role and that the interference of $\rho(770)^0$ and $f_0(500)$ also contributes significantly [14]. The CPVs, correspondingly, get contribution from the interference of the tree and penguin parts of the S- or P-wave amplitudes, which are in fact the origin of direct CPAs of the decay channel $B^\pm\to\pi^\pm f_0(500)$ or $B^\pm\to\pi^\pm\rho(770)^0$, and the interference between S- and P-waves amplitudes. All of the aforementioned contributions of CPV present in the regional CPAs, $A_{CP}^{\Omega_i^+}$ and $A_{CP}^{\Omega_i^-}$. While for the region Ω_i, the contribution from the S- and P-waves interfering term cancel out totally. Meanwhile, theoretical analysis in Sec. III shows that the (direct-CPV-subtracted) FB-CPAs contain only the contributions from the interference between the S- and P-waves amplitudes. The large FB-CPAs and the direct-CPV-subtracted FB-CPAs in Fig. 4 indicates with no doubt that the CPVs corresponding to the interference between S- and P-waves amplitudes dominant in the $f_0(500)-\rho(770)^0$ interference region. This can also be seen from the numerical values of A_{CP}^{FB}, $\tilde{A}_{CP}^{FB}$, A_{CP}^{Ω}, $A_{CP}^{\Omega^+}$ and $A_{CP}^{\Omega^-}$, of the whole region presented in Table I, from which one can see that the A_{CP}^{FB} and $\tilde{A}_{CP}^{FB}$ are much larger than A_{CP}^{Ω}.

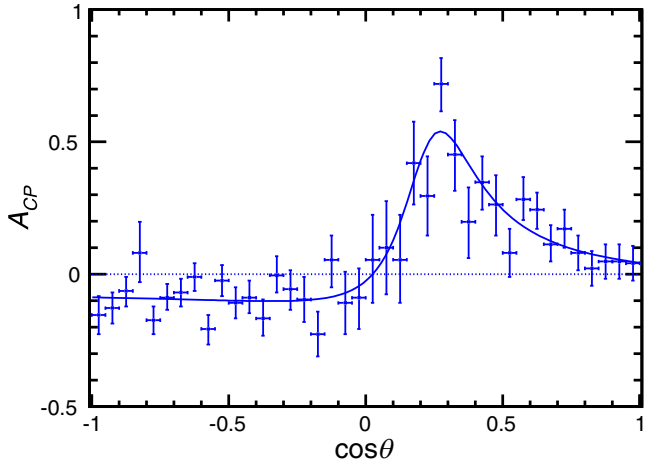

FIG. 5. Dependence of regional CPAs on $\cos\theta$ for 0.62 GeV/c^2 $<\sqrt{s_{\rm low}}<$ 0.78 GeV/c^2, where $\cos\theta$ is divided into 30 bins. The fitted curve is also shown in this figure.

The interference of the S- and P-waves can also explain the fine structures of the $\cos\theta$-dependencies of the regional CPAs. Figure 5 presents the $\cos\theta$-dependencies of the regional CPAs measured by LHCb for 0.62 GeV/c^2 $<\sqrt{s_{\rm low}}<$ 0.78 GeV/c^2, where $\cos\theta$ is equally divided into 30 bins [14]. From Fig. 5 one can clearly see that the regional CPAs depend on $\cos\theta$ strongly. It has been pointed out that the tendency of the regional CPAs of taking opposite signs for $\cos\theta>0$ and $\cos\theta<0$ is due to the interference of $f_0(500)$ and $\rho(770)^0$ [13]. Indeed, one can fit the data in Fig. 5 quite well by the inclusion of only $f_0(500)$ and $\rho(770)^0$. The fitted curve is also shown in Fig. 5.

To fit the data, the decay amplitude is parametrized as

$$\mathcal{A}_{B^-\to\pi^-\pi^+\pi^-}=\cos\theta\mathcal{R}_1\frac{c_\rho e^{i\delta_\rho}}{s_{\rm low}-m_\rho^2+im_\rho\Gamma_\rho}+\mathcal{R}_2\frac{c_f e^{i\delta_f}}{s_{\rm low}-m_f^2+im_f\Gamma_f},\tag{9}$$

$$\bar{\mathcal{A}}_{\mathcal{B}^+\to\pi^-\pi^+\pi^+}=\cos\theta\mathcal{R}_1\frac{\bar{c}_\rho e^{i\bar{\delta}_\rho}}{s_{\rm low}-m_\rho^2+im_\rho\Gamma_\rho}+\mathcal{R}_2\frac{\bar{c}_f e^{i\bar{\delta}_f}}{s_{\rm low}-m_f^2+im_f\Gamma_f},\tag{10}$$

where c_i and δ_i $(i=\rho,\ f)$ represent the corresponding amplitudes and the relative phases contribution of component $\rho(770)^0$ and $f_0(500)$, respectively, $\mathcal{R}_1=\sqrt{s_{\rm low}-m_\pi^2}\sqrt{\frac{(m_B^2-s_{\rm low}+m_\pi^2)^2}{s_{\rm low}}-m_\pi^2}$, $\mathcal{R}_2=\sqrt{s^*-m_\pi^2}\times\sqrt{\frac{(m_B^2-s^*+m_\pi^2)^2}{s^*}-m_\pi^2}$, where $s^*=\frac{m_\rho^2+m_f^2}{2}$ and m_B, m_π, m_ρ, and m_f are the masses of B, π, $\rho(770)^0$, and $f_0(500)$, respectively. The parameters used in Eqs. (9) and (10) are listed in Table II, and are borrowed from Ref. [34]. Our fit

TABLE II. Input parameters used in Eqs. (9) and (10).

Parameters	Value (in GeV)
$m_{B^\pm}$	5.279
m_π	0.139
$m_{\rho(770)^0}$	0.775
$\Gamma_{\rho(770)^0}$	0.149
$m_{f_0(500)}$	0.563
$\Gamma_{f_0(500)}$	0.350

TABLE III. Parameters values obtained by the fitting.

Parameter	Value	Parameter	Value
c_ρ	1	$\bar{c}_\rho$	1.05 ± 0.02
δ_ρ	0	$\bar{\delta}_\rho$	0
c_f	0.49 ± 0.07	$\bar{c}_f$	0.50 ± 0.06
δ_f	-0.64 ± 0.06	$\bar{\delta}_f$	-1.36 ± 0.31

is performed in a least square method. To fit the data, the three parameters c_ρ, δ_ρ, and $\bar{\delta}_\rho$ are set fixed at $c_\rho = 1$, $\delta_\rho = \bar{\delta}_\rho = 0$. The fitting results for the rest five of the parameters are presented in Table III. The goodness for this fit is $\chi^2/\text{d.o.f.} = 1.10$, where χ^2 is the Pearson's chi-square and is defined as $\chi^2 \equiv \sum_{j=1} \frac{(O_j - E_j)^2}{E_j}$ with O_j and E_j being the observed and expected event yields of bin j, and d.o.f. is the degrees of freedom.

IV. SUMMARY AND CONCLUSION

In this paper, the FBA, the FB-CPA, the direct-CPV-subtracted FB-CPAs and the regional CPAs for the three-body decay of B meson $B^\pm \to \pi^\pm\pi^+\pi^-$ are analyzed based on the data of LHCb [13,14]. We focus on the CPAs in the $f_0(500) - \rho(770)^0$ interfering region. It is found that the FB-CPAs are quite large in this region. According to the theoretical analysis, the large FB-CPA and the direct-CPV-subtracted FB-CPAs can be explained by the interference of the amplitudes corresponding to $f_0(500)$ and $\rho(770)^0$. Moreover, the analysis indicates that the interference between the amplitudes of $f_0(500)$ and $\rho(770)^0$ is the main contribution to CPVs in this region. The aforementioned interference can even explain more detailed structures of CPVs in this region, according to the fitting result of Fig. 5.

In conclusion, the interference of intermediate resonances can play an important role in CPV of three-body decay of bottom meson. The FB-CPA and the direct-CPV-subtracted FB-CPA, according the theoretical analysis and the data-based analysis of this paper, are ideal observables to study CPVs coursed by the interference of intermediate resonances.

ACKNOWLEDGMENTS

This work was supported by National Natural Science Foundation of China under Grant No. 12192261, and Natural Science Foundation of Hunan Province under Grant No. 2022JJ30483.

[1] J. H. Christenson, J. W. Cronin, V. L. Fitch, and R. Turlay, Evidence for the 2π Decay of the K_2^0 Meson, Phys. Rev. Lett. **13**, 138 (1964).
[2] A. D. Sakharov, Violation of CP Invariance, C asymmetry, and baryon asymmetry of the universe, Pis'ma Zh. Eksp. Teor. Fiz. **5**, 32 (1967).
[3] Nicola Cabibbo, Unitary Symmetry and Leptonic Decays, Phys. Rev. Lett. **10**, 531 (1963).
[4] Makoto Kobayashi and Toshihide Maskawa, CP violation in the renormalizable theory of weak interaction, Prog. Theor. Phys. **49**, 652 (1973).
[5] A. Alavi-Harati *et al.* (KTeV Collaboration), Observation of Direct CP Violation in $K_{S,L} \to \pi\pi$ Decays, Phys. Rev. Lett. **83**, 22 (1999).
[6] Bernard Aubert *et al.* (*BABAR* Collaboration), Observation of CP Violation in the B^0 Meson System, Phys. Rev. Lett. **87**, 091801 (2001).
[7] Kazuo Abe *et al.* (Belle Collaboration), Observation of Large CP Violation in the Neutral B Meson System, Phys. Rev. Lett. **87**, 091802 (2001).
[8] A. Poluektov *et al.* (Belle Collaboration), Evidence for direct CP violation in the decay $B^\pm \to D^{(*)}K^\pm$, $D^- \to K_S^0\pi^+\pi^-$ and measurement of the CKM phase ϕ_3, Phys. Rev. D **81**, 112002 (2010).
[9] P. del Amo Sanchez *et al.* (*BABAR* Collaboration), Measurement of CP observables in $B^\pm \to D_{CP}K^\pm$ decays and constraints on the CKM angle γ, Phys. Rev. D **82**, 072004 (2010).
[10] R Aaij *et al.* (LHCb Collaboration), First Observation of CP Violation in the Decays of B_s^0 Mesons, Phys. Rev. Lett. **110**, 221601 (2013).
[11] Roel Aaij *et al.* (LHCb Collaboration), Observation of CP Violation in Charm Decays, Phys. Rev. Lett. **122**, 211803 (2019).
[12] R Aaij *et al.* (LHCb Collaboration), Measurement of CP Violation in the Phase Space of $B^\pm \to K^\pm\pi^+\pi^-$ and $B^\pm \to K^\pm K^+ K^-$ Decays, Phys. Rev. Lett. **111**, 101801 (2013).
[13] Roel Aaij *et al.* (LHCb Collaboration), Measurements of CP violation in the three-body phase space of charmless $B^\pm$ decays, Phys. Rev. D **90**, 112004 (2014).
[14] Roel Aaij *et al.* (LHCb Collaboration), Amplitude analysis of the $B^+ \to \pi^+\pi^+\pi^-$ decay, Phys. Rev. D **101**, 012006 (2020).
[15] Roel Aaij *et al.* (LHCb Collaboration), Direct CP violation in charmless three-body decays of $B^\pm$ mesons, arXiv: 2206.07622.
[16] C. P. Jessop *et al.* (CLEO Collaboration), Study of Charmless Hadronic B Meson Decays to Pseudoscalar Vector Final States, Phys. Rev. Lett. **85**, 2881 (2000).
[17] A. Gordon *et al.* (Belle Collaboration), Study of $B \to \rho\pi$ decays at BELLE, Phys. Lett. B **542**, 183 (2002).

[18] Bernard Aubert *et al.* (*BABAR* Collaboration), An amplitude analysis of the decay $B^{\pm} \to \pi^{\pm}\pi^{\pm}\pi^{\mp}$, Phys. Rev. D **72**, 052002 (2005).

[19] Bernard Aubert *et al.* (*BABAR* Collaboration), Dalitz plot analysis of $B^{\pm} \to \pi^{\pm}\pi^{\pm}\pi^{\mp}$ decays, Phys. Rev. D **79**, 072006 (2009).

[20] Zhen-Hua Zhang, Xin-Heng Guo, and Ya-Dong Yang, CP violation in $B^{\pm} \to \pi^{\pm}\pi^{+}\pi^{-}$ in the region with low invariant mass of one $\pi^{+}\pi^{-}$ pair, Phys. Rev. D **87**, 076007 (2013).

[21] J. P. Dedonder, A. Furman, R. Kaminski, L. Lesniak, and B. Loiseau, S-, P- and D-wave $\pi\pi$ final state interactions and CP violation in $B^{\pm} \to \pi^{\pm}\pi^{\mp}\pi^{\pm}$ decays, Acta Phys. Pol. B **42**, 2013 (2011).

[22] J. H. Alvarenga Nogueira, I. Bediaga, A. B. R. Cavalcante, T. Frederico, and O. Lourenço, CP violation: Dalitz interference, CPT, and final state interactions, Phys. Rev. D **92**, 054010 (2015).

[23] I. Bediaga and P. C. Magalhães, Final state interaction on $B^{+} \to \pi^{-}\pi^{+}\pi^{+}$, arXiv:1512.09284.

[24] Zhen-Hua Zhang, Ren Song, Yu-Mo Su, Gang Lu, and Bo Zheng, Theoretical analysis of direct CP violation and differential decay width in $D^{\pm} \to \pi^{\pm}\pi^{+}\pi^{-}$ in phase space around the resonances $\rho^{0}(770)$ and $f_{0}(500)$, Eur. Phys. J. C **75**, 401 (2015).

[25] Hai-Yang Cheng, Cheng-Wei Chiang, and Chun-Khiang Chua, Finite-width effects in three-body B decays, Phys. Rev. D **103**, 036017 (2021).

[26] Hai-Yang Cheng and Chun-Khiang Chua, Branching fractions and CP violation in $B^{-} \to K^{+}K^{-}\pi^{-}$ and $B^{-} \to \pi^{+}\pi^{-}\pi^{-}$ decays, Phys. Rev. D **102**, 053006 (2020).

[27] Zhen-Hua Zhang, A novel observable for CP violation in multi-body decays and its application potential to charm and beauty meson decays, Phys. Lett. B **820**, 136537 (2021).

[28] Rui Hu and Zhen-Hua Zhang, Data-based analysis of the forward-backward asymmetry in $B^{\pm} \to K^{\pm}K^{\mp}K^{\pm}$, Phys. Rev. D **105**, 093007 (2022).

[29] Roel Aaij *et al.* (LHCb Collaboration), Measurement of B^{0}, B_{s}^{0}, B^{+} and Λ_{b}^{0} production asymmetries in 7 and 8 TeV proton-proton collisions, Phys. Lett. B **774**, 139 (2017).

[30] Zhen-Hua Zhang, Analysis of the angular distribution asymmetries and the associated CP asymmetries in bottom baryon decays, arXiv:2208.13411.

[31] Jian-Peng Wang and Fu-Sheng Yu, Probing hyperon CP violation from charmed baryon decays, arXiv:2208.01589.

[32] The Belle Collaboration, Measurement of branching fractions and decay asymmetry parameters for $\Lambda_{c}^{+} \to \Lambda h^{+}$ and $\Lambda_{c}^{+} \to \Sigma^{0}h^{+}$ ($h = K$, π), and search for CP violation in baryon decays, arXiv:2208.08695.

[33] William Elwood Byerly, *An Elementary Treatise on Fourier's Series and Spherical, Cylindrical, and Ellipsoidal Harmonics* (Dover Publications, New York, 2003).

[34] R. L. Workman (Particle Data Group), Review of particle physics, Prog. Theor. Exp. Phys. **2022**, 083C01 (2022).